TELKOMNIKA, Vol.17, No.6, December 2019, pp.3232~3248
ISSN: 1693-6930, accredited First Grade by Kemenristekdikti, Decree No: 21/E/KPT/2018
DOI: 10.12928/TELKOMNIKA.v17i6.13224

A photovoltaic integrated unified power quality conditioner with a 27-level inverter

Kamel Saleh*[1], Naeil Hantouli[2]
Electrical Engineering Department, An-Najah National University, Nablues-West Bank, Palestine
*Corresponding author, e-mail: kamel.saleh@najah.edu[1], naeil_hantouli@yahoo.com[2]

Abstract

This paper presents a Unified Power Quality Conditioner (UPQC) with a 27-level inverter based on an asymmetric H-bridge topology. Each phase of the inverter is composed of three H-bridges, supplied by three DC sources scaled in the power of three. The output of the multilevel inverter is connected directly to the point of common coupling (PCC) without the need to a transformer or a filter. The calculation of the Shunt Active Power Filter (SAPF) compensation current is based on the generalized theory of synchronous frame (d-q theory) while the calculation of a series active filter voltage is based on Instantaneous Reactive Power (p-q theory). The control of the SAPF is achieved by using a closed-loop vector control followed by a new multilevel modulation technique. In addition to the capability of harmonic elimination of both current and voltage drawn from the source, the UPQC can produce real and reactive power to feed the loads during prolonged voltage outages or source shortage. Batteries pack are used as a dc link, which is charged from photovoltaic array connected to the battery through a maximum power point tracker and charge controller. The injection of real and reactive power depends on the state of charge (SOC) of batteries, the frequency of the system, real and reactive power of the load, and power factor at the point of PCC. The proposed UPQC strategy is simulated in MATLAB SIMULINK and the results have shown a significant improved in Total Harmonics Distortion (THD) of both the voltage and currents.

Keywords*: active filters, multilevel inverter, solar power generation*

1. Introduction

In last decades, the uses of the power electronics devices have been increased significantly in many fields such as adjustable speed drives [1], arc furnaces [2], electric vehicle battery chargers [3], lighting equipment such as compact fluorescent and LED lamps [4] and in renewable energy sources. Despite its benefits [5], the uses of power electronics devices shifted the electrical loads from linear to non-linear i.e. producing harmonic currents [6]. These harmonics can cause a severe effect on the whole power system such as causing overheating in transmission lines and transformer and male function of protection devices. Therefore, harmonic elimination has been of extensive concern and investigation. To eliminate harmonic pollution, passive filters were applied. These filters have many drawbacks such as: bulky, only capable of compensating a limited range of harmonics and they can produce resonance phenomena when connected to the power grid [7]. On the other hand (Active power filter (APF) has many advantages, such as high filtering accuracy, superior dynamic response, modularity and scalability, making it an ideal device to compensate harmonics and improve power quality [8, 9]. APFs are considered the second stage of development and an effective solution to overcome the limitation of PFs. However, the size, cost, and rating of APFs are considerably increased by the increasing demand for power system capacity [10, 11]. To overcome the issues of shunt APFs, the third stage of development consists of hybrid power filter (HPF) devices which comprise hybrid combinations of PFs with shunt APFs [12]. Furthermore, HPF technology is evaluated in the fourth stage of development as a unified power quality conditioner (UPQC) [13]. Several control theories for APFs have been developed and described in the literature, with the p-q theory [14], the FBD [15], the CPC [16] and the synchronous reference frame d-q theory [17] being among the main methods for obtaining the compensation currents for APFs.

Regarding its structure, an APF is a DC-AC power converter, which can be either of the voltage source type or the current source type [18]. Moreover, a DC-AC power converter can be also classified by the number of levels of the output voltage or current, whereby it is considered

Received May 29, 2019; Revised July 2, 2019; Accepted July 18, 2019

a multilevel converter if the number of levels is three or more [19]. Multilevel converters are advantageous for medium voltage applications since they are capable of providing higher output voltages than the voltage that power semiconductors have to withstand. Besides, multilevel converters produce less dv/dt and have a better performance in terms of Total Harmonic Distortion (THD) when compared to two-level converters [20]. There are three classical topologies of multilevel converters, namely the neutral point clamped (or diode clamped) [21], the flying capacitor (or capacitor clamped) [22], and the cascaded multilevel converter [23]. Nevertheless, several topologies have been proposed in the literature, aiming to achieve higher numbers of levels with reduced switch counts [24–29]. Accordingly, control and modulation techniques for multilevel converters have been also widely investigated [30, 31].

The objective of this paper is to show the advantages of using UPQC that is using multilevel inverter and battery storage. Compared to conventional PWM techniques, this converter, in any of its functionalities, able to produce current waveforms with negligible harmonic content. To produce active power, the system uses a battery pack kept charged using photovoltaic arrays. Furthermore, the batteries can also be charged from the mains when required. The paper describes the topology of the system and show simulations with a small 13-kVA prototype. The results demonstrate the ability of active filters to compensate harmonics in voltages and current in addition to compensate reactive power. Moreover, the paper shows the ability of such a filter to be used as a renewable energy source to support the grid in high-demand hours.

2. Research Method

2.1. Descriptin of PV-UPQC System

2.1.1. Basic Principle

The power circuit of the three-phase PV-UPQC system is shown in Figure 1. The APF is using a 27-level asymmetrical inverter. Each phase of this inverter consists of three H-bridges supplied by three independent photovoltaic arrays. A 125 w polycrystalline PV modules (Mitsubishi Electric PV-EE125MF5F) have been used to design all photovoltaic arrays. These photovoltaic arrays are delivering 12.5 kva to each phase, 10 kva for shunt active filter and 2.5 kva for the series active filter as shown in Table 1.

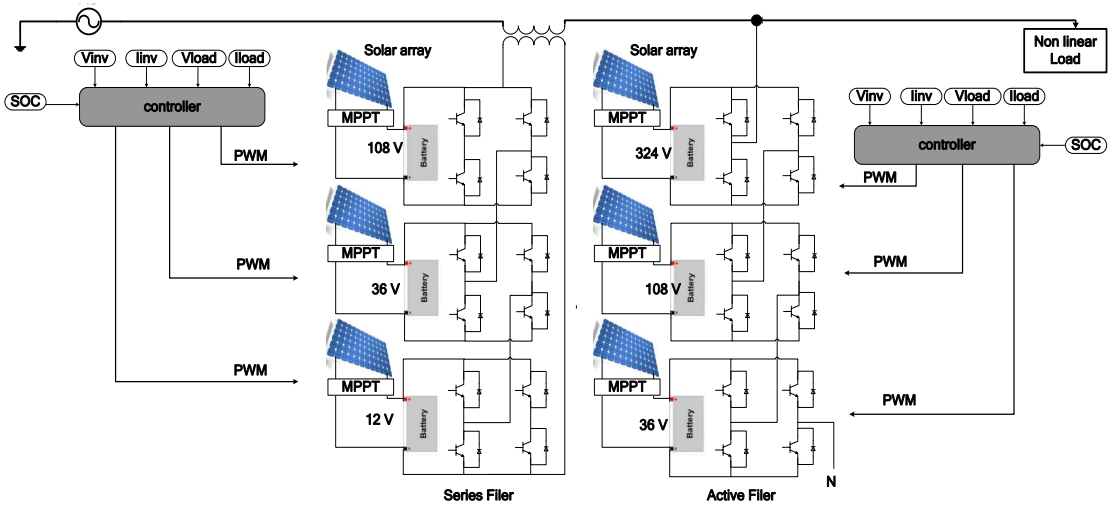

Figure 1. Power circuit structure of the PV-UPQC system

Battery packs are used as dc link and charged from photovoltaic array connected to the battery through a maximum power point tracker and charge controller. Table 2 shows the details of the battery packs used for the series and shunt filters. The output of the shunt active filter is connected directly to the transmission line at a PCC while the series active filter is connected to the transmission line through a coupling transformer. In addition to the capability of harmonic elimination of both current and voltage drawn from the source, the combined system can produce real and reactive power to feed the loads during prolonged voltage outages or source

shortage. The injection of real and reactive power depends on the state of charge (SOC) of batteries, real and reactive power of the load, and power factor at the point of common coupling (PCC).

Table 1. The Combinations of PV Module for Designing Photovoltaic Arrays Sources

	Shunt Filter			Series Filter		
	Combination	Power(w)	(%)	Combination	Power(w)	Percent (%)
AUX.1	1 in series*4 in parallel	500	5%	1 in series*1 in parallel	125	5%
AUX.2	3 in series*4 in parallel	1500	15%	1 in series*3 in parallel	375	15%
MAIN	11 in series*6 in parallel	8000	80%	4 in series*4 in parallel	2000	80%
Total (w)	10 kw			2.5 kw		

Table 2. The Per Phase Combinations of Battery Packs

	Shunt Filter			Series Filter		
	Combination	AH	Voltage(v)	Combination	AH	Voltage(v)
AUX.1	3 in series*4 in parallel	400	36	1 in series*1 in parallel	100	12
AUX.2	9 in series*4 in parallel	400	108	1 in series*3 in parallel	100	36
MAIN	27 in series*7 in parallel	700	324	4 in series*4 in parallel	175	108
Total (w)	10 kw			2.5 kw		

2.1.2. Multi-level Inverter

A symmetric cascaded multi-level inverter is used in this research [31]. Each leg of the inverter consists of three H-bridges connected in series and supplied by three independent photovoltaic arrays scaled in the power of three as shown in Figure 2. This configuration of the multi-level inverter helps to generate 27-level at the output of the inverter instead of generating 7 levels when using symmetric sources. The output of each H-bridge is shown in Figure 2. It can be noted that the switching frequency of the main H-bridge, which manages more than 80% of the total power, is the same frequency of the system, in this case, only 50 Hz. The frequency of the auxiliary H-Bridges are also low but increases as the voltage level of the inverter become lower in the chain. The total harmonic distortion of the output waveform of the multilevel inverter is only 1.8% while it is in the case of using 2-level inverter is 5.4%. This low THD at the output of the multi-level helps to get ride of the need for any kind of filtering at the output of the active filter.

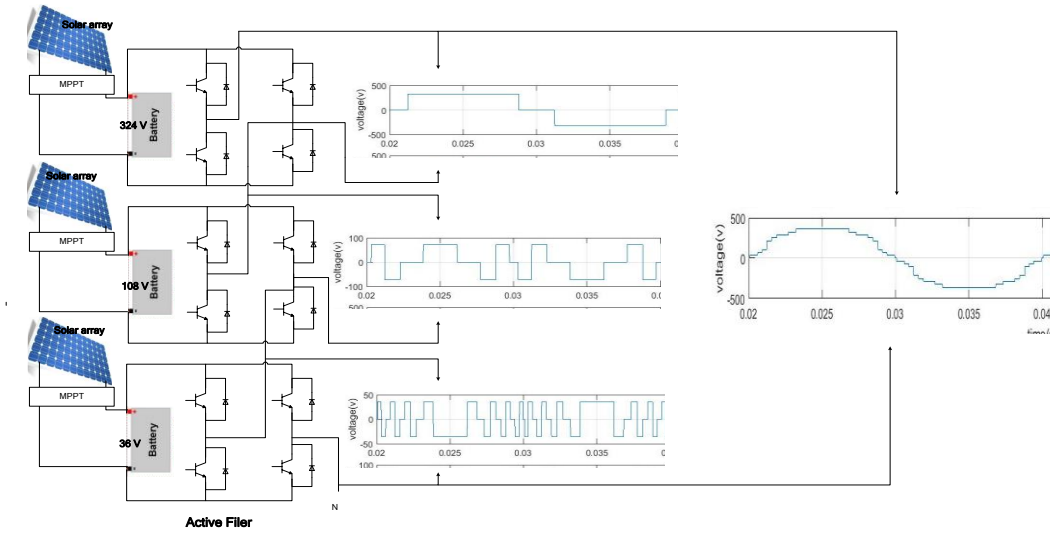

Figure 2. Asymmetric 27-level inverter

2.2. Control Scheme

Many techniques were introduced in the literature to calculate the reference currents and voltgaes for active filters [14, 15, 17]. These currents and voltages will have all the components

of the current and voltage that needed to be compensated by the active filter to achieve unity power factor and minimum distortion in both voltage and current of the source.

2.2.1. Reference Current Calculation for Shunt Active Filter

Synchronous Reference d-q method was adopted in this research to calculate the current reference for active filter [14]. The algorithm of this method is illustrated in Figure 3. This method based on transforming the load current into the load voltage synchronous frame d-q frame. In such a case the current will have two components Id and Iq. The Id current is in the direction of the load voltage and so it is the real power current component. The Iq current will be perpendicular to the load voltage and hence it is the reactive power current component.

These d-q current components will have two components. The first component is the dc component that represents the fundamental component of the real and reactive components. The ac component represents the harmonics in the current. Moreover, the injection of real power from the PVs can be done by adding a component to Id as shown in Figure 3.

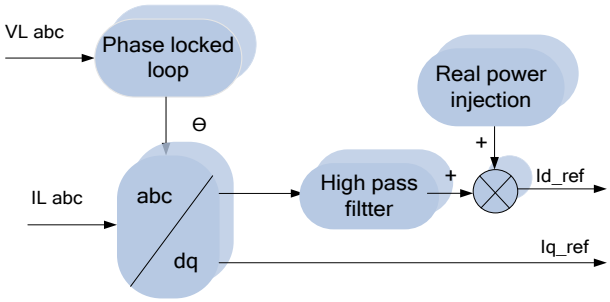

Figure 3. Principle of instantaneous active and reactive power theory (d-q method)

2.2.2. Refrence Voltage Valculation for Series Active Filter

The instantaneous real and reactive method (PQ method) is adopted in this research to calculate the reference voltages for the series active filter [17]. This technique is illustrated in Figure 4. The output components Vα_ref and Vβ_ref are the harmonic components in the voltages that are needed to filter out using the series active filter.

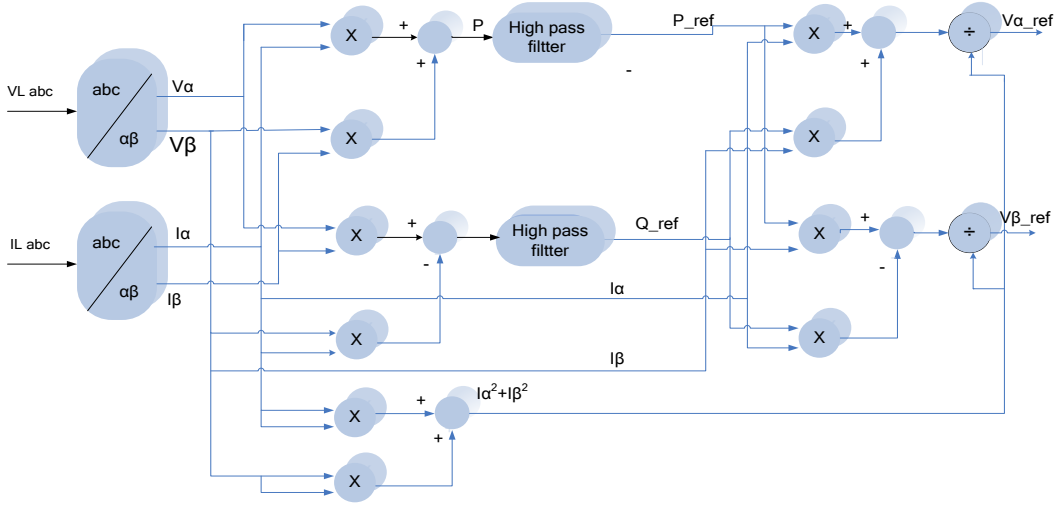

Figure 4. Principle of instantaneous active and reactive power theory (P-Q method)

2.2.3. Control of Active Power Injection for Shunt Active Filter

The injection of the active power (P) injected to the point of common coupling (PCC) depends on the SOC of all battery packs and the system frequency to ensure the stability of

the electrical network as shown in Figure 5. The control system will measure the state of charge (SOC) of all batteries and the network frequency then output a signal to a multilevel inverter controller contains the optimum value of real power need to be injected. If the SOC of any battery less than or equal 0.28, this state called empty or fault battery state, then the system will charge the batteries at a maximum rate to push the state of charge (SOC) from an empty region to charging region. And If the state of charge (SOC) of all batteries greater than 0.35, and the frequency of the system is normal i.e. between 49.5 and 50.5, this state is called normal state and the system will charge the batteries at a rate that guarantee fully charged batteries at the end of sunset. During the charging process, the excessive power from PV arrays will be injected to the electrical distribution network directly by setting the real power reference current (id) according to the excessive power from the charging process.

When the state of charge (SOC) is greater than 0.5 and the frequency of the system is less than 49.5, this state called unstable network state. The system will stop charging batteries and inject all power that comes from PV arrays, also discharges the batteries at rated discharging current, by setting the real power reference current (id) according to the maximum power available. If the frequency of the system is greater than 0.5, or no real power load at distribution network then this state called non-real power load state, the system will stop power injection and charges the batteries only, by setting the real power reference current (id) to zero. These reference currents Id_ref and Iq_ref will be used then by the controller.

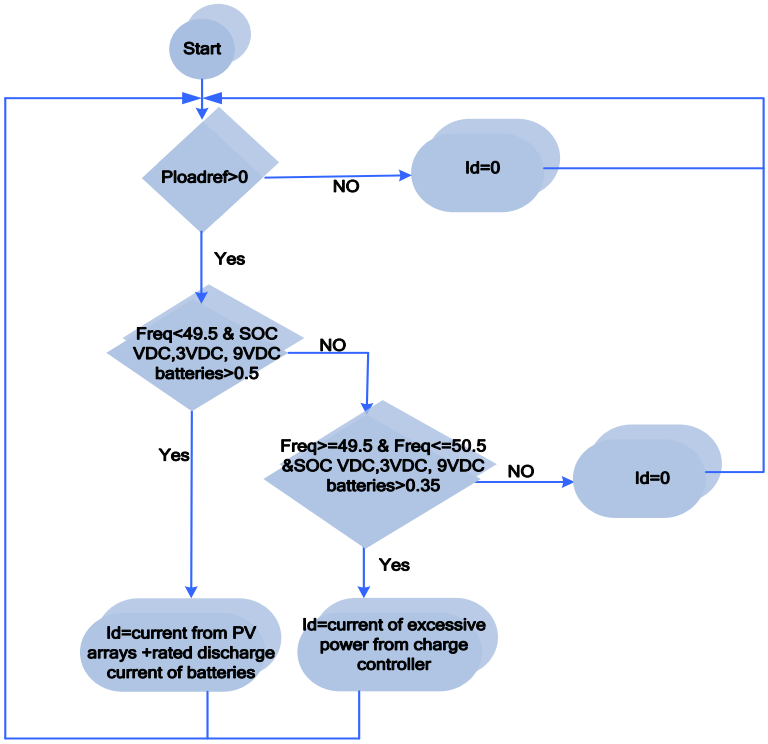

Figure 5. The flowchart diagram of active power control algorithm

2.2.4. Control of Reactive Power Injection for Shunt Active Filter

The injection of reactive power (Q) is only necessary when the load draws reactive power from the source. In the case of empty batteries, the system will disconnect the batteries from the dc link and continue reactive power compensation by inserting of capacitor banks at the dc link of each “H” bridge inverter. So the reactive power injection did not depend on the state of charge (SOC) of batteries, this will increase the reliability of the hybrid active filter to support the reactive power load even if no power generated from photovoltaic arrays. The flowchart diagram of the control algorithm is shown in Figure 6. When there is no load connected to the source the reactive power current reference (iq_ref) set to zero and no reactive power injected to the point of common coupling (PCC). And if reactive load is connected to

the distribution network, the system will automatically generate iq-ref required for all reactive power loads connected, and the source will see a unity power factor independent on the type of contaminating the load.

The speed of compensation of reactive power depending on the power factor of the electrical network, so if the power factor (PF) is less than 0.85 (lagging), the system compensates at maximum available reactive power, else the system will inject the excessive power from charging process. According to the above explanation, the system works like a synchronous machine, where the reactive power is controlled through the excitation coil. In this case, it is controlled through iq_ref.

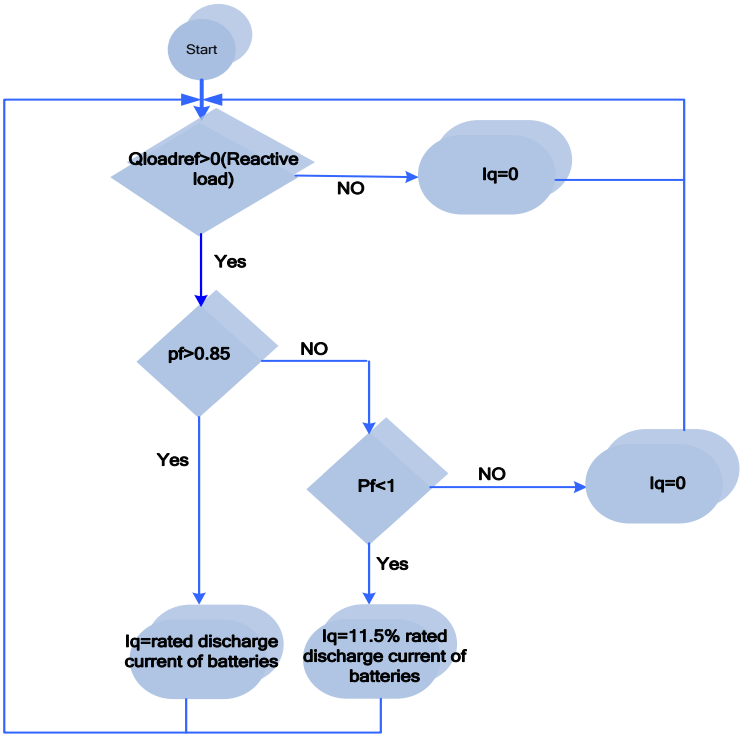

Figure 6. The flowchart diagram of reactive power control algorithm

2.2.5. Modelling and Control of Shunt Active Filter

Assume that the active filter is connected to the PCC through a resistance and inductance as shown in Figure 7. The following equations hold true:

$$vinva = ifaRf + Lf\frac{difa}{dt} + vpcca \quad (1)$$

$$vinvb = ifbRf + Lf\frac{difb}{dt} + vpccb \quad (2)$$

$$vinvc = ifcRc + Lf\frac{difc}{dt} + vpccc \quad (3)$$

All (1), (2), and (3) are transformed in terms of the d-q variables using the reference frame transformation as follows:

$$\mathrm{Lf}\frac{\mathrm{difd}}{\mathrm{dt}} = -\mathrm{ifdRf} + (\mathrm{Vinvd} - \mathrm{Vpccd}) - \omega\mathrm{Lf\,ifq} \quad (4)$$

$$\mathrm{Lf}\frac{\mathrm{difq}}{\mathrm{dt}} = -\mathrm{ifqRf} + (\mathrm{Vinvq} - \mathrm{Vpccq}) + \omega\mathrm{Lf\,ifd} \quad (5)$$

both (4) and (5) can be rewritten as:

$$vd = ifdRf + Lf\frac{difd}{dt} \quad (6)$$

$$vq = iqfRf + Lf\frac{difq}{dt} \quad (7)$$

where

$$vd = (Vinvd - Vpccd) - \omega Lf\, iq \quad (8)$$

$$vq = (Vinvq - Vpccq) + \omega Lf\, id \quad (9)$$

both (8) and (9) are used then to design a proportional-integral controller (PI) to control the id and iq components of the inverter currents as shown in Figure 8. The output of the controllers (Vdq) is then used to generate pulses for the IGBTs in the multi-level inverter as shown in Figure 9.

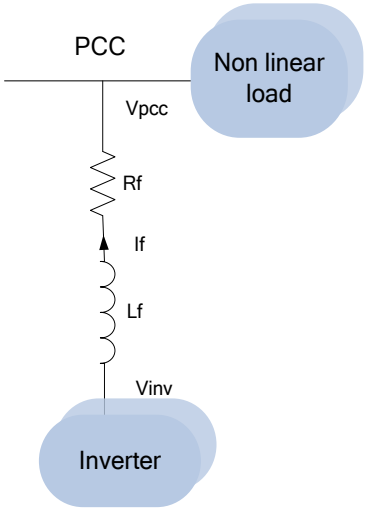

Figure 7. Dynamic modelling of the shunt active filter

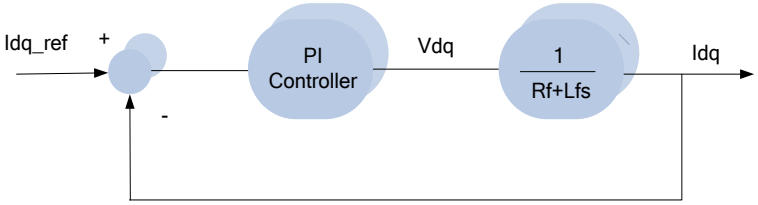

Figure 8. Closed loop control block diagram for shunt active filter

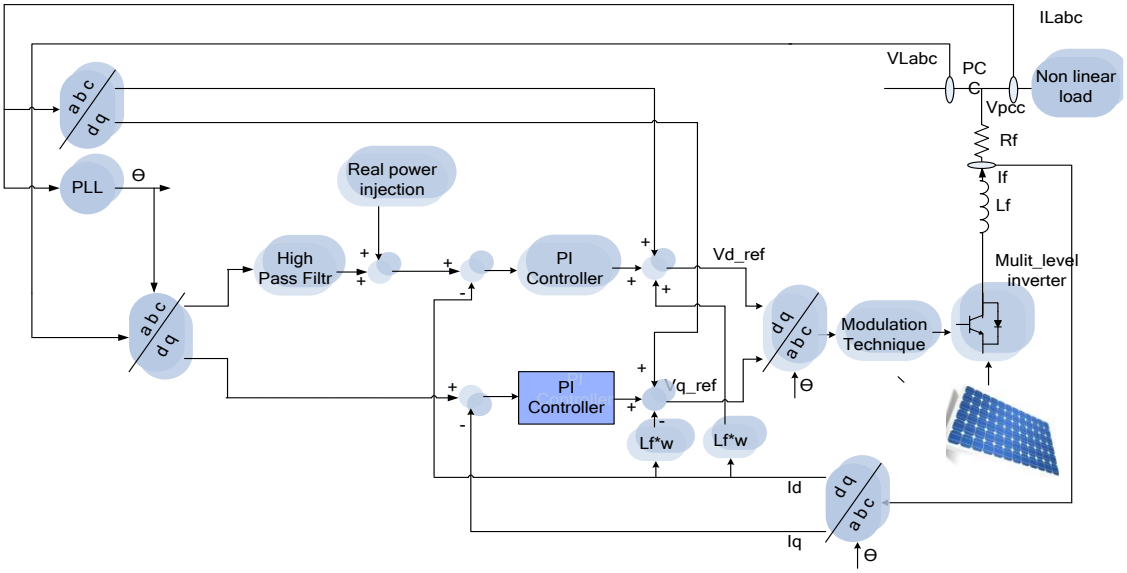

Figure 9. The control structure of active filter

3. Results and Analysis

The proposed system is simulated in MATLAB SIMULINK environment to check the performance and the correct working of the complete system. The simulation of Unified Power Quality Conditioner (UPQC) is tested to insure the correct working of all system parts composed together.

3.1. Simulation Results for Shunt Active Filter

Figure 10 shows the source current before and post the operation of the active filter. At t = 0.4 s the active power filter starts working to mitigate the harmonics and the source current became pure sinusoidal. The total harmonic distortion (THD) reduced from 18% to 0.4%. Then at t = 0.7 s, the active power injection starts with 6 A current assistant as seen in Figure 10 and the total harmonic distortion remained very low (0.5%) during active power injection.

3.2. Simulation Results for Series Active filter

The three-phase source voltage signal is shown before and post the operation of the series active filter is shown in Figure 11. At t = 0.4 s the series active filter started to mitigate the voltage harmonics. Then At t = 0.7 s, the system steps up the source voltage to 230 v and made the electrical network ideal with total harmonic distortion 1% in source voltage. It is clear from the above results, the behavior of Series APF became better and the capability of harmonic mitigation and voltage compensation became ideal because of the positive effect of shunt APF.

3.3. Power Factor Correction

Figure 12 proves the capability of shunt active power filter (SAPF) of keeping a unity power factor at the source. At t = 0.4 s, the shunt active filter starts to inject reactive power and the power factor has been improved from 0.78 to 0.97. Then at t = 0.7 s the active filter starts to inject real power the results in Figure 12 demonstrate that the power factor correction process hasn't been interrupted by the real power injection process.

3.4. Real Power Injection

The active power (P) was controlled by adjusting the value of id-ref current, where id-ref current depends on the SOC of all battery packs and the frequency of the system. The injection of reactive power (Q) depends on the tuning of iq-ref current, where iq-ref set to maintain a unity power factor. Figure 13 shows the changing in source current when the system starts active power injection at t = 0.7 sec. The injection of real power has been stopped at t = 0.9 s and the source current returns to its previous value before the real power injection.

3.5. Frequency Variation Effect

Figures 14 and 15 demonstrate the effect of the frequency variation on the amount of the real power injected by the filter. At t = 0.5 s When the network frequency between the normal limits (between 49.5 Hz and 50 Hz), the system adjusts id-ref to inject real power with a certain value depending on the state of charge (SOC) of batteries as shown in Figure 14. Figure 15 demonstrates the current injection when the frequency in the normal region, id-ref is set to 15% of the rated id. On the other hand, if the SOC is set to 0.9 (for example) and the network frequency down suddenly to 48 Hz at t = 0.7 s, the controller will adjust id-ref to its maximum value and push the network frequency to the normal region as shown in Figures 14 and 15. The total harmonic distortion (THD) is reduced from 16.5% to 1% and did not change when the controller injects different levels of current to the point of common coupling. Hence the system is trusted and stable for all its tasks.

3.6. State of Charge (SOC) Variation Effect

Figures 16 and 17 show the effect of changing the SOC on id-ref and the amount of real power injected by the active filter. Figure 16 shows that the state of charge has been declined from 0.8 to 0.25 at t=0.7 s. The three-phase source current waveforms are shown in Figure 17. At t=0.5 s the SOC was 0.8 so the controller set the value of id_ref to the maximum as shown in Figure 17. Then at t=0.7 s the SOC was declined to 0.25 and hence the controller set id_ref to 0 as shown in Figure 17.

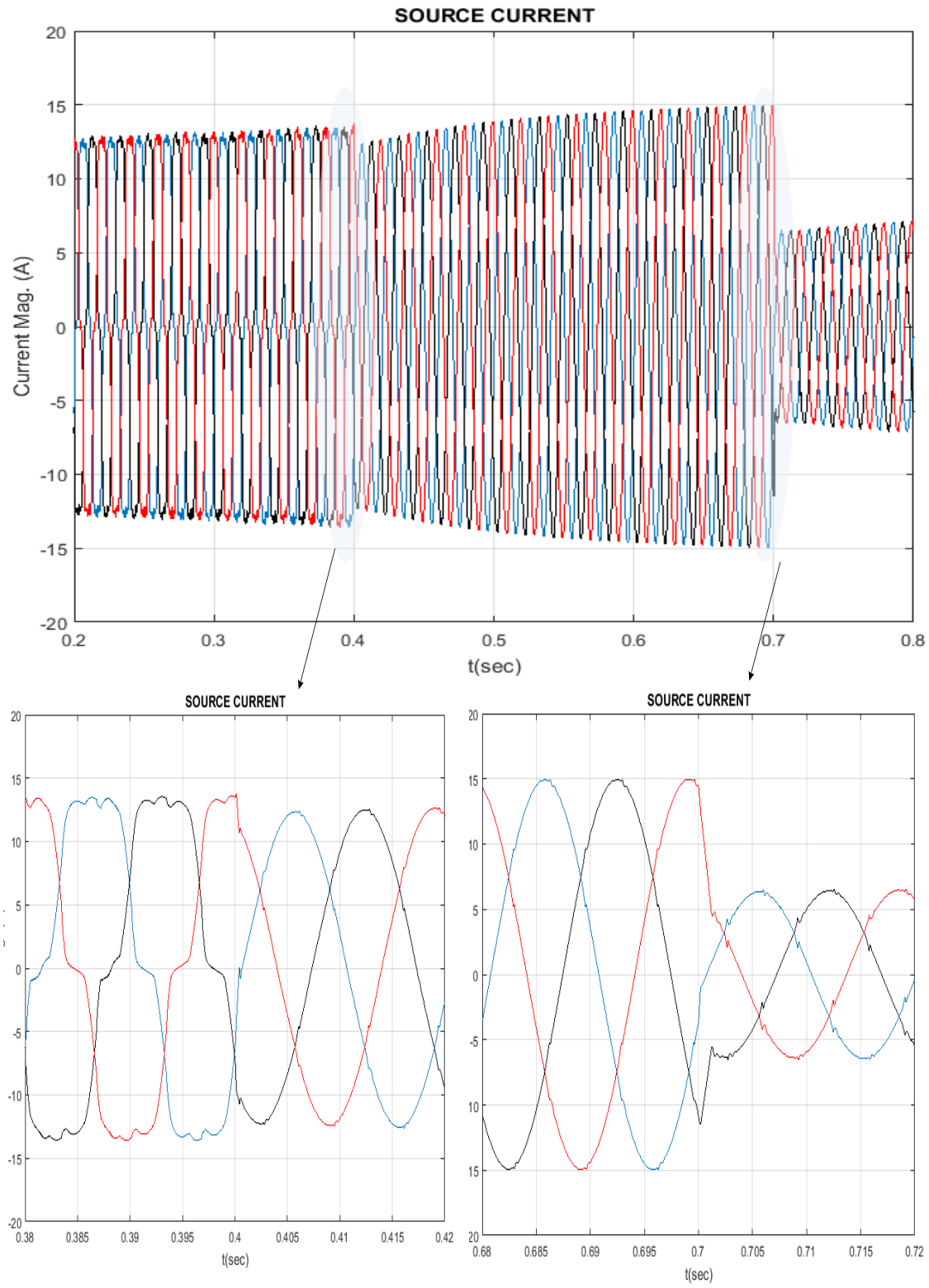

Figure 10. Source current waveforms after operation of active filter

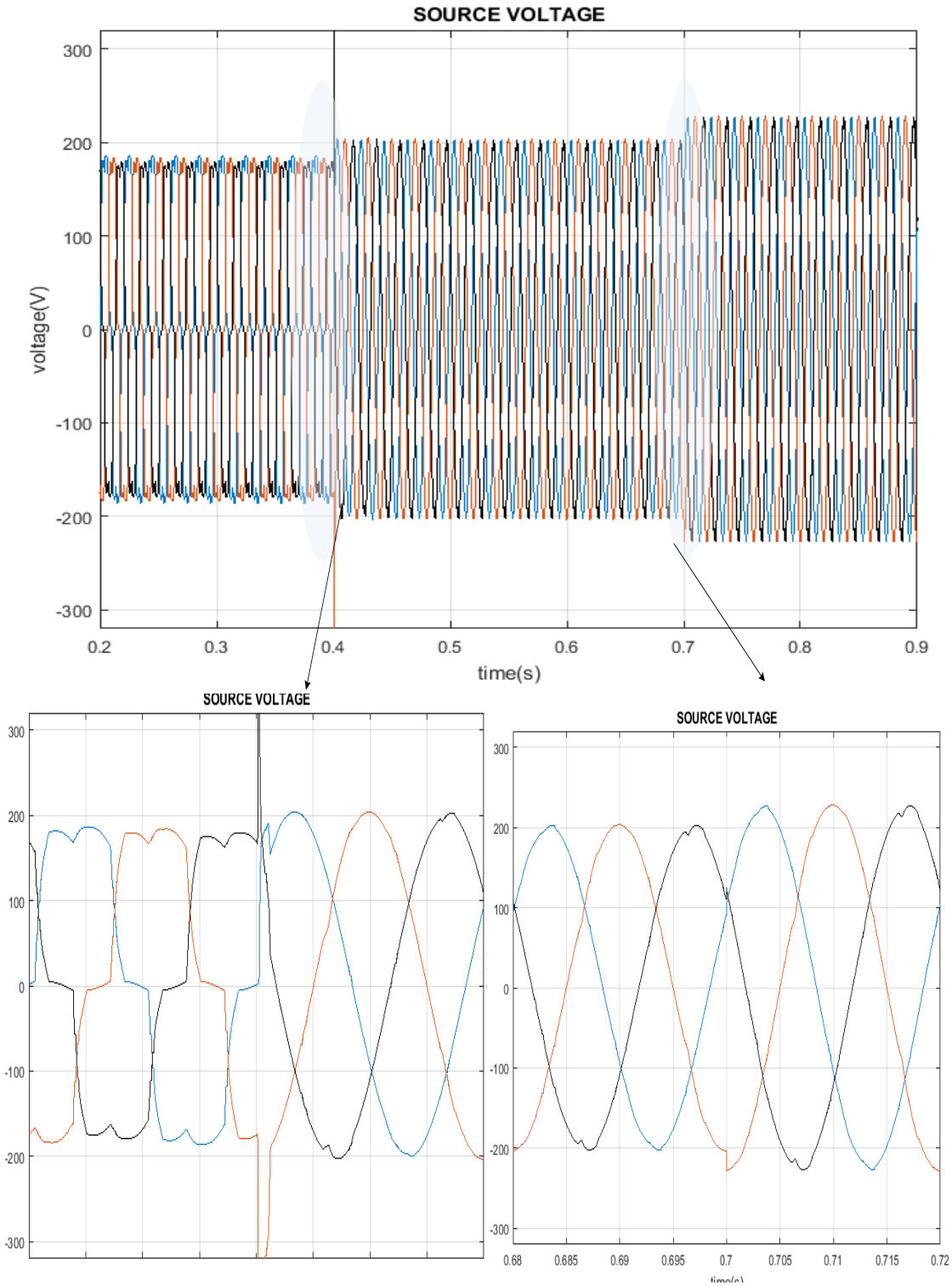

Figure 11. Source voltage waveforms after operation of series active filter

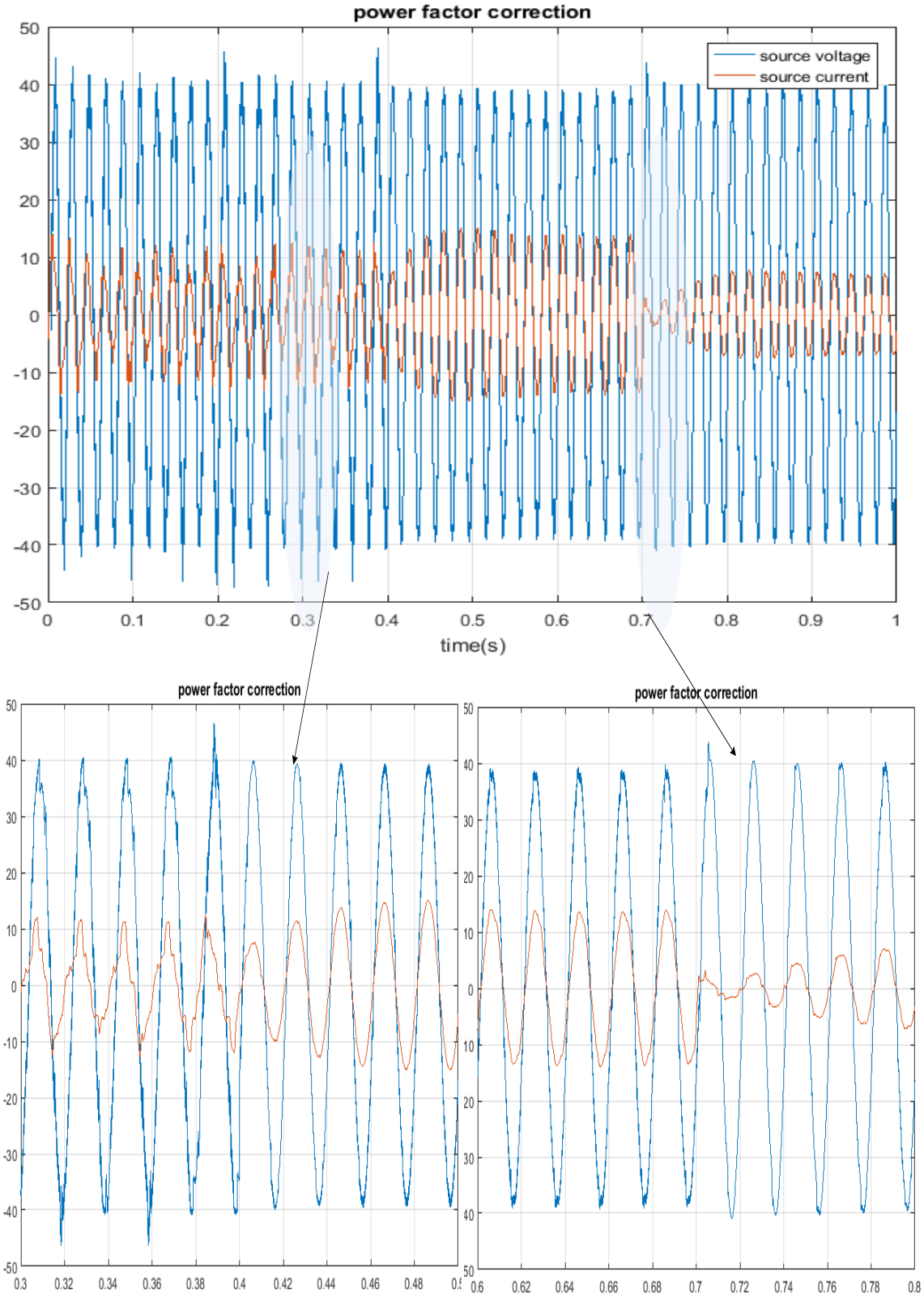

Figure 12. Source current waveform after reactive power injection using active filter

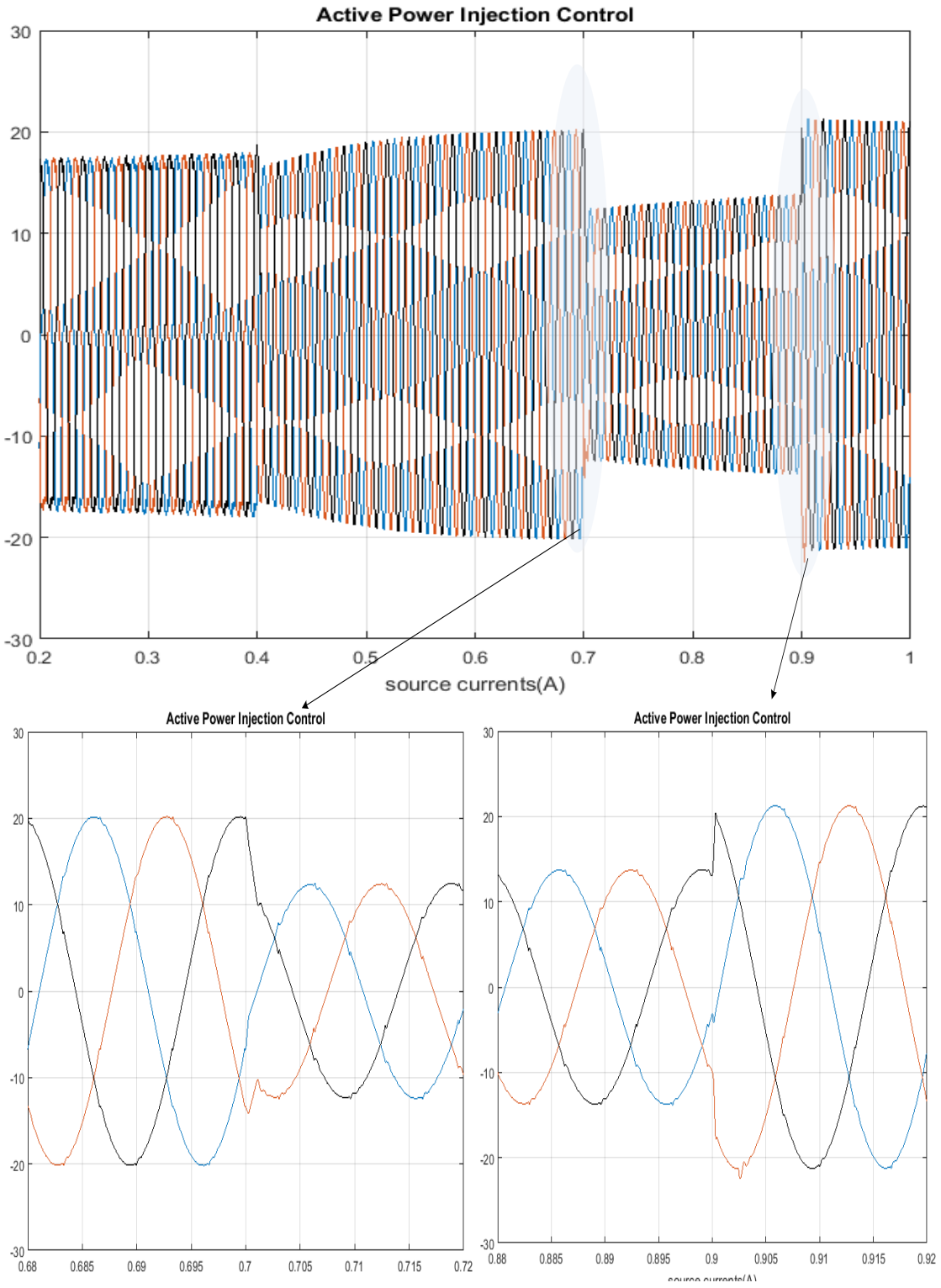

Figure 13. Source current waveforms after real power injection

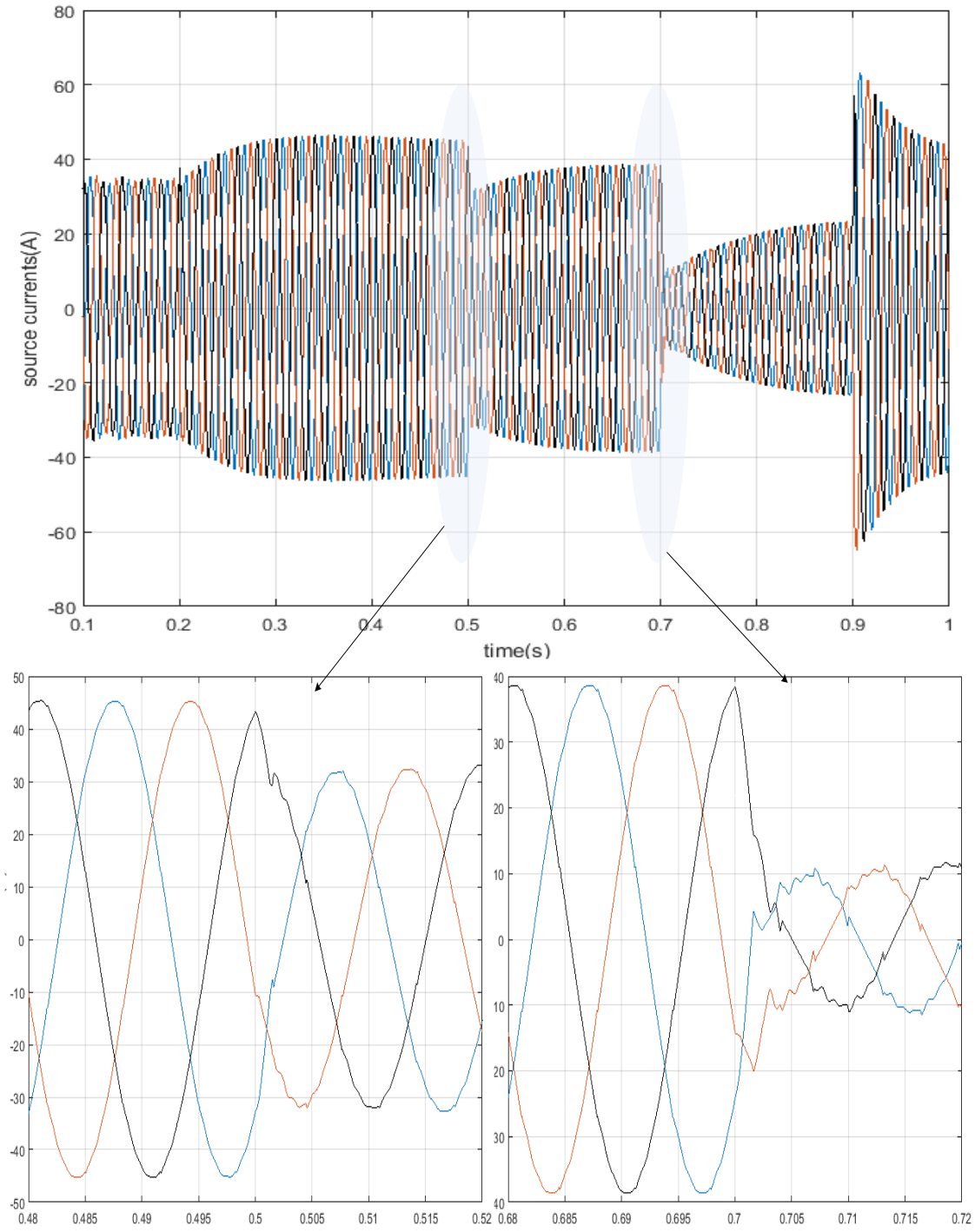

Figure 14. Three phase source current waveform under
different real power injection levels depending on the frequency

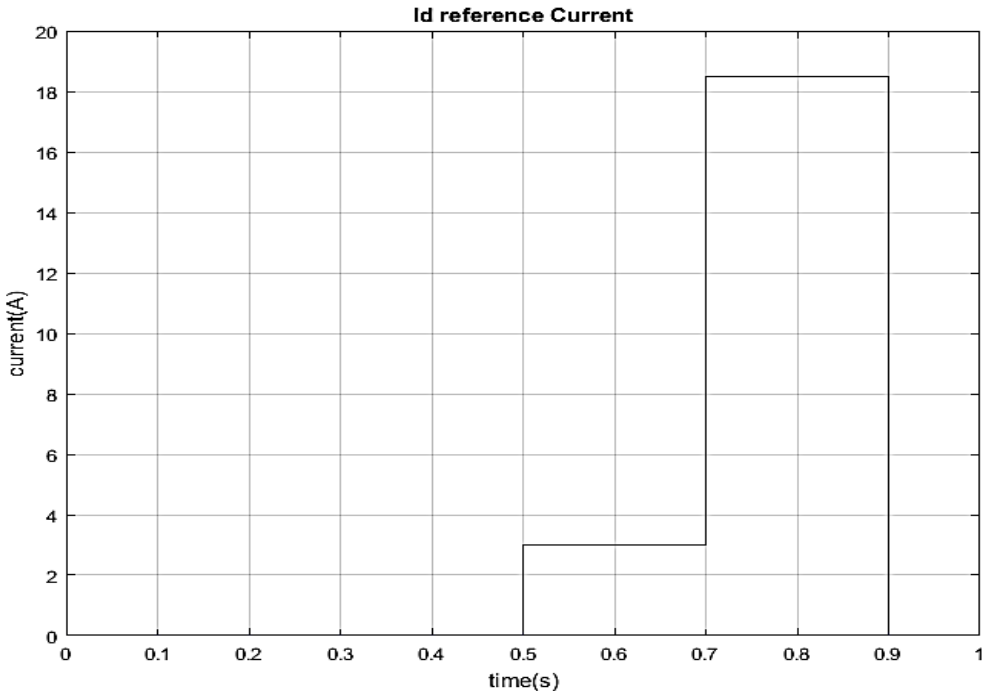

Figure 15. Changing in id reference current depending on the frequency range

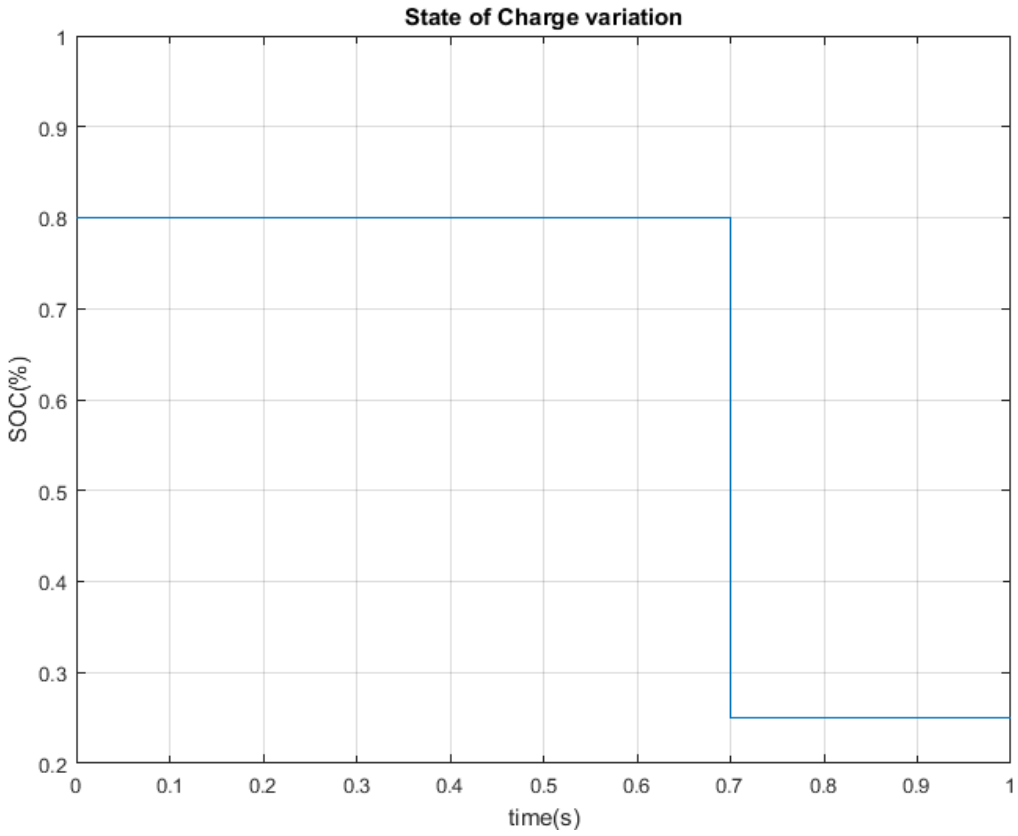

Figure 16. The state of charge variation

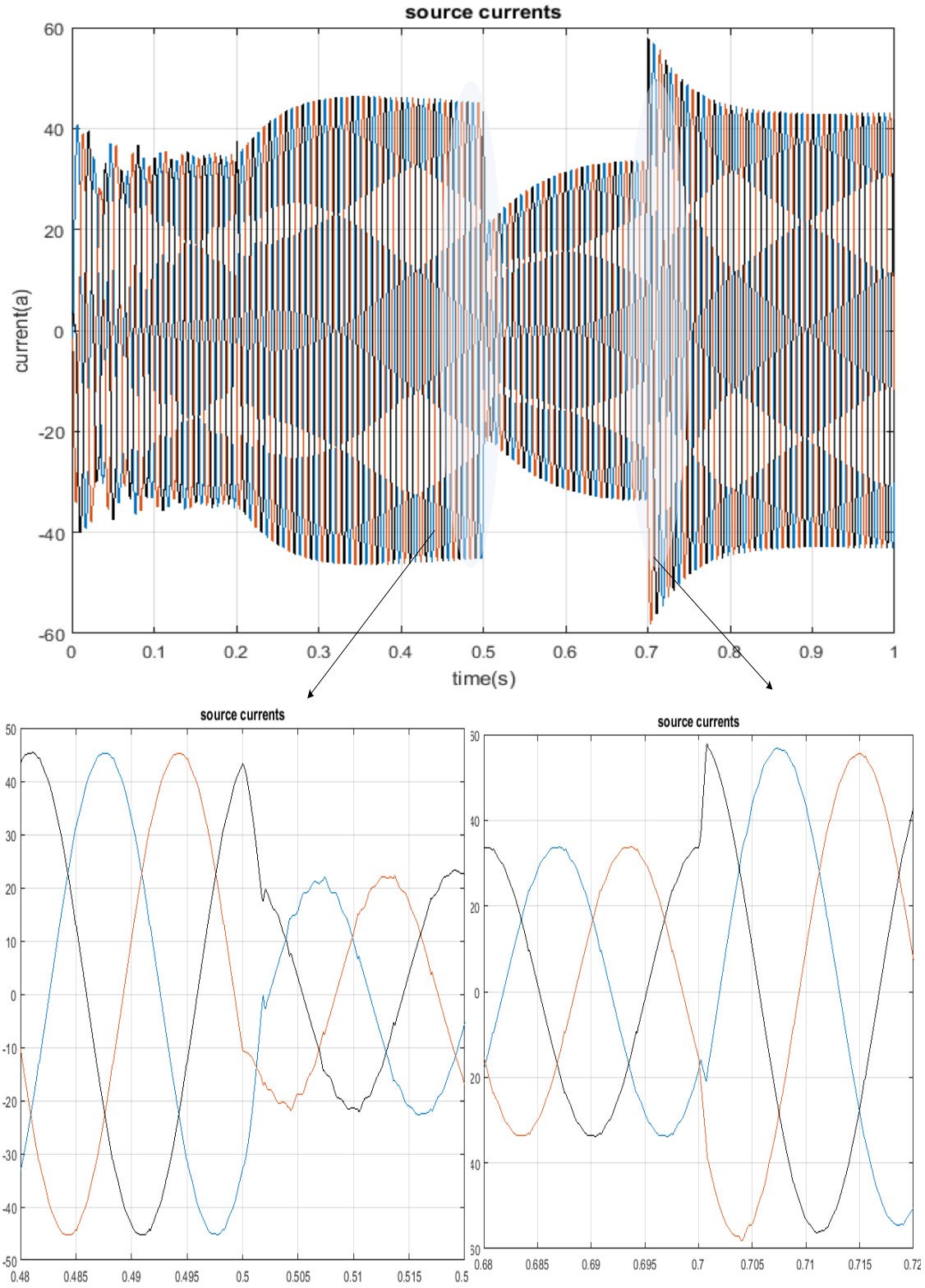

Figure 17. Three phase source current waveform under
different real power injection levels depending on the SOC

4. Conclusion

This paper has introduced a Unified Power Quality Conditioner (UPQC) integrated with Photovoltaic and using a multi-level converter. In addition to the capability to inject reactive power and filtering the harmonics, the UPQC has the capability to inject real power depending on the frequency and the state of charge of batteries. The multilevel inverter that is used has the ability to generate 27 levels that help to reduce the THD in the source currents and voltages significantly with the need for any extra filters.

References

[1] Lee K, Carnovale D, Young D, Ouellette D, Zhou J. System Harmonic Interaction Between DC and AC Adjustable Speed Drives and Cost Effective Mitigation. *IEEE Trans. Ind. Appl*. 2016; 52(4): 3939–3948.
[2] Mendis SR, Gonzalez DA. Harmonic and transient overvoltage analyses in arc furnace power systems. *IEEE Trans. Ind. Appl*. 1992; 28(2): 336–342.
[3] Gomez JC, Morcos MM. Impact of EV battery chargers on the power quality of distribution systems. *IEEE Trans. Power Deliv*. 2003; 18(3): 975–981.
[4] Blanco AM, Stiegler R, Meyer J. *Power Quality Disturbances Caused by Modern Lighting Equipment (CFL and LED)*. IEEE Grenoble Conference. Grenoble, France. 2013: 1–6.
[5] Hoene E, Deboy G, Sullivan CR, Hurley G. Outlook on Developments in Power Devices and Integration: Recent Investigations and Future Requirements. *IEEE Power Electron. Mag*. 2018; 5(1): 28–36.
[6] IEEE Standards Association. 519-1992. *IEEE Recommended Practices and Requirements for Harmonic Control in Electrical Power Systems*. New York: IEEE Press. 1993.
[7] Peng FZ, Akagi H, Nabae A. A new approach to harmonic compensation in power systems-a combined system of shunt passive and series active filters. *IEEE Trans. Ind. Appl*. 1990; 26(6): 983–990.
[8] Palmer JA, Degeneff RC, McKernan TM, Halleran TM. Pipe-type cable ampacities in the presence of harmonics. *IEEE Trans. Power Deliv*. 1993; 8(4): 1689–1695.
[9] Faiz J, Ghazizadeh M, Oraee H. Derating of transformers under non-linear load current and non-sinusoidal voltage—An overview. *IET Electron. Power Appl*. 2015: 9(7): 486–495.
[10] Lam CS, Choi WH, Wong MC, Han YD. Adaptive DC-Link Voltage-Controlled Hybrid Active Power Filters for Reactive Power Compensation. *IEEE Trans. Power Electron*. 2012; 27(4): 1758–1772.
[11] Espi J, Garcia-Gil R, Castello J. Capacitive Emulation for LCL-Filtered Grid-Connected Converters. *Energies*. 2017; 10(7): 930.
[12] Litran SP, Salmeron P. Analysis and design of different control strategies of hybrid active power filter based on the state model. *IET Power Electron*. 2012; 5(8): 1341–1350.
[13] Mahela OP, Shaik AG. A Topological aspect of power quality improvement techniques: A comprehensive overview. *Renew. Sustain. Energy Rev*. 2016; 58: 1129–1142.
[14] Akagi H, Kanazawa Y, Nabae A. *Generalized Theory of the Instantaneous Reactive Power in Three-Phase Circuits*. International Power Electronics Conference. Japan. 1983: 1375–1386.
[15] Depenbrock M. The FBD-method, a generally applicable tool for analyzing power relations. *IEEE Trans. Power Syst*. 1993; 8(2): 381–387.
[16] Czarnecki LS. Orthogonal decomposition of the currents in a 3-phase nonlinear asymmetrical circuit with a nonsinusoidal voltage source. *IEEE Trans. Instrum. Meas*. 1988; 37(1): 30–34.
[17] Bhattacharya S, Divan D. *Synchronous frame-based controller implementation for a hybrid series active filter system*. IEEE Industry Applications Conference Thirtieth IAS Annual Meeting. USA. 1995; 3: 2531–2540.
[18] Pinto JG, Exposto B, Monteiro V, Monteiro LFC, Couto C, Afonso JL. *Comparison of current-source and voltage-source Shunt Active Power Filters for harmonic compensation and reactive power control*. IECON 2012—38th Annual Conference on IEEE Industrial Electronics Society. Canada. 2012: 5161–5166.
[19] Lai J, Peng FZ. *Multilevel converters-a new breed of power converters*. IAS Annual Meeting. USA. 1995: 2348–2356.
[20] Rodriguez J, Lai J, Peng FZ. Multilevel inverters: A survey of topologies, controls, and applications. *IEEE Trans. Ind. Electron*. 2002; 49(4): 724–738.
[21] Nabae A, Takahashi I, Akagi H. A New Neutral-Point-Clamped PWM Inverter. *IEEE Trans. Ind. Appl*. 1981; IA-17(5): 518–523.
[22] Hochgraf C, Lasseter R, Divan D, Lipo TA. *Comparison of multilevel inverters for static VAr compensation*. IEEE Industry Applications Society Annual Meeting. USA. 1994: 921–928.
[23] Teodorescu R, Blaabjerg F, Pedersen JK, Cengelci E, Enjeti PN. Multilevel inverter by cascading industrial VSI. *IEEE Trans. Ind. Electron*. 2002; 49(4): 832–838.

[24] Hasan M, Abu-Siada A, Islam S, Muyeen S. A Novel Concept for Three-Phase Cascaded Multilevel Inverter Topologies. *Energies*. 2018; 11: 268.
[25] Reddy KBM, Pattnaik S. *Novel symmetric and asymmetric topology of multilevel inverter with reduced number of switches*. IEEE International Conference on Industrial Technology (ICIT). Canada. 2017: 165–170.
[26] Elias MFM, Rahim NA, Ping HW, Uddin MN. *Asymmetrical transistor-clamped H-bridge cascaded multilevel inverter*. IEEE Industry Applications Society Annual Meeting. USA. 2012: 1–8.
[27] Dixon J, Moran L. High-level multistep inverter optimization using a minimum number of power transistors. *IEEE Trans. Power Electron*. 2006; 21(2): 330–337
[28] Haddad M, Rahmani S, Hamadi A, Al-Haddad K. *New Single Phase Multilevel reduced count devices to Perform Active Power Filter*. Proceedings of the SoutheastCon. USA. 2015: 1–6.
[29] Martinez-Rodrigo F, Ramirez D, Rey-Boue A, de Pablo S, Lucas LH. Modular Multilevel Converters: Control and Applications. *Energies*. 2017; 10: 1709.
[30] Moranchel M, Huerta F, Sanz I, Bueno E, Rodríguez F. A Comparison of Modulation Techniques for Modular Multilevel Converters. *Energies*. 2016; 9: 1091.
[31] Flores P, Dixon J, Ortuzar M, Carmi R, Barriuso P, Moran L. Static Var Compensator and Active Power Filter With Power Injection Capability, Using 27-Level Inverters and Photovoltaic Cells. *IEEE Transactions on Industrial Electronics*. 2009; 56(1): 130-138.